Emulsion Synthesis of Nanoparticles Containing PEDOT Using Conducting Polymeric Surfactant: Synergy for Colloid Stability and Intercalation Doping

CHI-AN DAI,[1,2] CHUN-JIE CHANG,[2] HUNG-YU CHI,[1] HUNG-TA CHIEN,[1] WEI-FANG SU,[2] WEN-YEN CHIU[1,2]

[1]Department of Chemical Engineering, National Taiwan University, Taipei, 106 Taiwan, Republic of China

[2]Institute of Polymer Science and Engineering, National Taiwan University, Taipei, 106 Taiwan, Republic of China

ABSTRACT: Poly(3,4-ethylenedioxythiophene): poly(styrenesulfonate) (PEDOT:PSS) is a widely used conductive aqueous dispersion synthesized by using emulsion polymerization method. To further enhance its solution processability and conductivity of PEDOT derivatives, we proposed to replace the nonconductive PSS with conductive poly[2-(3thienyl)-ethoxy-4-butylsulfonate] (PTEB) as surfactant for the emulsion polymerization of PEDOT. The reaction involved colloid stabilization and doping in one step, and yielded PEDOT:PTEB composite nanoparticles with high electrical conductivity. Contrary to its counterpart containing nonconductive surfactant, PEDOT:PTEB showed increasing film conductivity with increasing PTEB concentration. The result demonstrates the formation of efficient electrical conduction network formed by the fully conductive latex nanoparticles. The addition of PTEB for EDOT polymerization significantly reduced the size of composite particles, formed stable spherical particles, enhanced thermal stability, crystallinity, and conductivity of PEDOT:PTEB composite. Evidence from UV–VIS and FTIR measurement showed that strong molecular interaction between PTEB and PEDOT resulted in the doping of PEDOT chains. X-ray analysis further demonstrated that PTEB chains were intercalated in the layered crystal structure of PEDOT. The emulsion polymerization of EDOT using conducting surfactant, PTEB demonstrated the synergistic effect of PTEB on colloid stability and intercalation doping of PEDOT during polymerization resulting in significant conductivity improvement of PEDOT composite nanoparticles. © 2008 Wiley Periodicals, Inc. J Polym Sci Part A: Polym Chem 46: 2536–2548, 2008

Keywords: conducting polymer; emulsion polymerization; nanoparticles

INTRODUCTION

Poly(3,4-ethylenedioxythiophene)s (PEDOT) represent a class of conjugated polymers that can be potentially used as active materials for flexible organic electronics because of their superior conductivity, transparency and thermal stability.[1–3]

Their unique optoelectronic properties make PEDOT an excellent material for various applications such as in electrochromics,[4] antistatic coating,[5] light emitting diodes,[6,7] solar cell,[8,9] sensors,[10–13] and biotechnology.[14,15] The optoelectronic properties of PEDOT can be further tailored by controlling its synthetic processes,[16–18] altering the polymer backbone conformation,[19,20] changing different dopant types,[21,22] and introducing various functional groups onto its main chain.[23,24] However, since pure PEDOT bulk

material is insoluble and infusible, much research attention has been focused on the development of a solution-processable PEDOT formulation. Currently, a commercially available aqueous dispersion solution of PEDOT and poly (styrenesulfonate) (PEDOT-PSS, trade name Baytron®) was developed by the Bayer AG Company of Germany. PSS serves as charge balancing dopant during polymerization.[25] Although PEDOT-PSS is solution processable, there are problems associated with the formulation for applications that require low surface resistance and high optical transparency.[26,27] For example, the conductivity of the PEDOT-PSS film is significantly lower than that of pure PEDOT. In addition, water is not particularly a good solvent for spin coating to attain large uniform films. Although electrochemical polymerization is widely used to fabricate conductive polymer thin films, the requirement of using a conducting substrate from which a conductive polymer is formed may be too restrictive to meet the needs for various applications.[28]

In order for mass production, the chemical oxidative polymerization of PEDOT is a promising alternative. Such method enables the deposition of films on substrates by a variety of methods such as spin-coating or knife casting. There have been various extensive researches made on the synthesis of PEDOT using chemical oxidative polymerization.[25,29–32] Among the chemical oxidative polymerization, emulsion polymerization seems to be most promising.[33,34] However, since the monomer, 3,4-ethylenedioxythiophene (EDOT) is relatively insoluble in water and the once-initiated monomer, for example, thienyl cation radicals reacts in water, a typical oil-in-water emulsifier-free emulsion polymerization of EDOT results in low yields and poor conductivity. To circumvent this problem, it has recently been suggested that adding surfactants such as small molecule surfactant, for example, sodium dodecyl sulfate (SDS) or polymeric surfactant, for example, poly (styrenesulfonate) to an aqueous solution of EDOT significantly improves polymerization yield.[35] The advantage of the use of surfactant containing sulfonate functional groups is that the surfactant stabilizes the synthesized colloids as well as doping in one step which yields PEDOT with high electrical conductivity. In general, the conductivity of the latex particle increases with increasing doping level of PEDOT from the sulfonate groups of the surfactant. However, with excess amount of the

nonconductive surfactants on the outer surface of conductive particles, the conductivity of the film made from the core-shell latex reaches a maximum and decreases with increasing surfactant amount.

To overcome the aforementioned problem, a typical oil-in-water emulsion polymerizations of PEDOT in the presence of water soluble conductive oligomers or polymers as surfactant may be useful. It has been shown previously that core-shell nanoparticles consisting of nonconductive polymer core and conductive shell of various types of conducting polymers for example, polypyrrole, polyaniline, and so forth can be prepared.[36–39] Emulsion polymerization has also been used to synthesize latex composite particles with multifunctionalities including sensor, magnetic, and electronic properties.[40,41] Although a small addition of conductive polymers was needed to form a conductive-filler network with a high electrical conductivity, further improvement in conductivity beyond a full coverage of the core surface with conductive polymer is limited.

In this article, we will present a strategy for preparing fully conductive latex nanoparticles using emulsion polymerization. We propose to synthesize a conductive polyanion, poly[2-(3thienyl)-ethoxy-4-butylsulfonate] (PTEB), as a surfactant for the emulsion polymerization of PEDOT. Since PEDOT chains are insoluble in water, they can be adsorbed and stabilized by PTEB chains to form composite latex particle. Since PTEB possesses conjugated structure which enables charge transport from one PEDOT domain to the other, we have found that the conductivity of the coated PEDOT:PTEB film increase with increasing amount of PTEB addition. In addition, the effects of addition of the conductive surfactant on the thermal property, crystallinity, and doping level of the composite nanoparticles were thoroughly studied.

EXPERIMENTAL

Materials

Thienyl ethanol, sodium hydride, 1,4-butanesulton, and tetrabutylammonium hydroxide (40 wt % solution in water) were used for the synthesis of PTEB and toluene was used as a solvent for the reaction. For PEDOT:PTEB latex synthesis, 3,4-ethylenedioxythiophene (EDOT) and iron
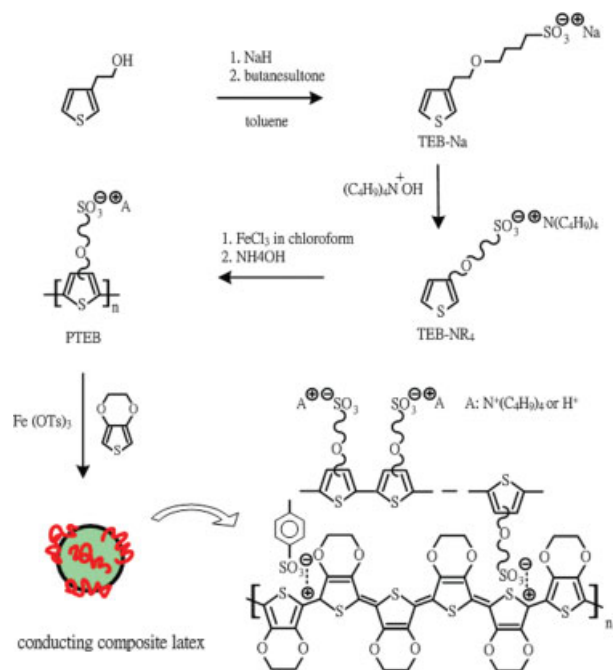
Figure 1. The synthesis scheme for conductive surfactant, PTEB, and emulsion synthesis scheme for PTEB/PEDOT core shell latex nanoparticles. PEDOT chains adsorb onto PTEB and form a composite nanoparticle.

(III) *p*-toluenesulfonate (Fe(OTs)$_3$) were purchased from Aldrich and used as received. Toluene was distilled to remove water before used while methanol was used as received.

Chemical Synthesis of TEB

The synthesis of poly[2-(3thienyl)-ethoxy-4-butylsulfonate] (PTEB) from thienyl ethanol was conducted according to the literature procedure.[39] 3-thienyl ethoxybutanesulfonic acid sodium salt (TEB-Na) was synthesized by ring opening of 1,4-butanesulton as shown in Figure 1. Since the polymerization of TEB-Na monomer in water gives low yield, Tran-Van et al. showed that by replacing sodium cation wtih tetrabutylammonium cation TEB-NR$_4$ has good solubility in chloroform and can be polymerized with FeCl$_3$ in chloroform to obtain high yield.[39] Figure 2(a,b) shows the H-NMR characterization of TEB-Na and subsequently modified TEB-NR$_4$ monomers, respectively. We performed a similar procedure and the polymerization was carried out under argon at room temperature for 24 h. After filtration, the black precipitate was washed with dichloromethane to remove unreacted monomers, iron(II),

chlorine(I), and other salts. The dark precipitate was then stirred in an excess amount of NH$_4$OH solution for 2 days to remove iron(III) by reacting with the basic solution to form insoluble iron(III) hydroxide and to exchange the iron(III) complexed with the sulfonate groups for ammonium ions. The solution turns red. After filtration the aqueous solution was evaporated to obtain a solid red-brown product in 70% yield.[39] PTEB of two different molecular weights was synthesized by adjusting the molar ratio of TEB monomer to the oxidant, FeCl$_3$ and the resulting PTEBs are denoted as L-PTEB and H-PTEB for low and high molecular weight, respectively. The weight-averaged molecular weight and the polydispersity index (PDI) of the PTEB are listed in Table 1.

Characterization

Surface Tension Measurement

Surface tensions of the PTEB solution were measured by a tensiometer (Kruss model no. K12). A sandblasted platinum plate with dimension of $24 \times 10 \times 0.2$ mm was used for surface tension measurement. The surface tension for each PTEB solution sample was averaged over three sets of measurements. The difference between the three measurements was usually within 3%.

Thermal Gravimetric Analysis

Thermal gravimetric analysis (TGA) was conducted to characterize the thermal stability of PTEB and PEDOT:PTEB latex samples using DuPont 951 from the room temperature to 600 °C with a heating rate of 10 °C/min under nitrogen atmosphere. The measurements were conducted using 5 mg samples. The weight retention versus temperature curves were recorded. Samples for the TGA measurement were first grinded then dried in an oven at 85 °C for a day prior to the measurement to prevent moisture absorption.

FTIR Measurement

The compositions and the doping level of PEDOT:PTEB latex particles were measured with a Fourier transform IR spectrometer (Jasco, FTIR-615R) using a pressed CaF$_2$ pellet technique.
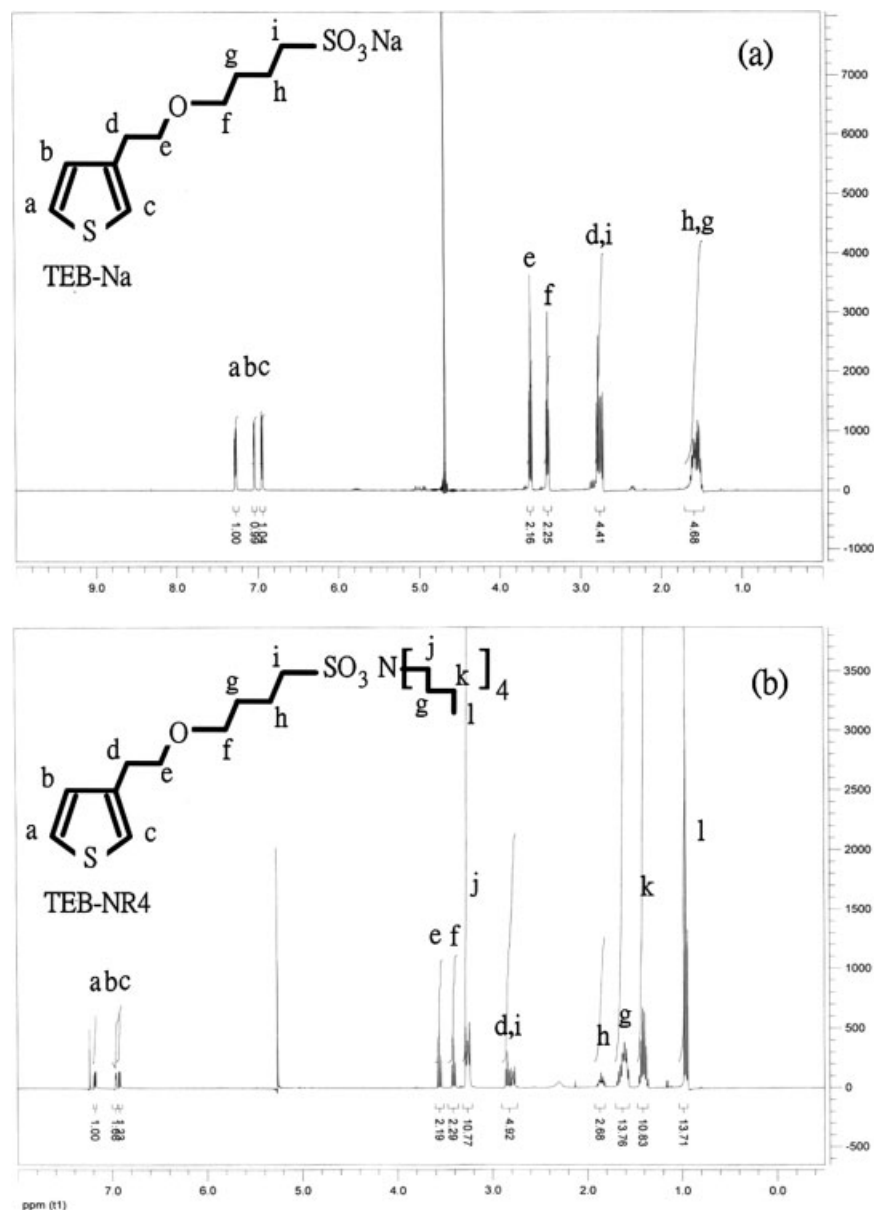
Figure 2. H-NMR measurement on (a) TEB-Na and (b) TEB-NR4 monomers.

Conductivity Measurement

The surface resistances of composite films were measured using a standard four-point probe method. The thickness of copolymer film was measured with a TENCOR α-Step 500 surface profiler. The film samples were prepared by knife coating the latex solution onto a glass substrate and subsequently drying the film in an oven at 40 °C for 12 h. The thickness of all films after drying was maintained to be around 20 μm. The conductivity, σ of copolymer film was calculated by the equation $\sigma = \frac{1}{Rd}$ where σ is the conductivity in S/cm, R is the surface re-sistance in Ω, and d is the thickness of copolymer film. To measure the UV–Visible absorption spectra, latex solutions were diluted to a concentration of 1×10^{-5} M of PEDOT:PTEB in water. The UV–Visible absorption spectra of the solution were recorded with a Helios UV–VIS spectrometer.

Transmission Electron Microscopy Measurement

To prepare samples for TEM observation, carbon-coated copper grids were used as substrates for drop coating a diluted latex solution on

Table 1. Characteristics of the Conducting Surfactant, PTEB, and the Corresponding PEDOT:PTEB Latex Particles

Sample ID	TEB:FeCl$_3$ Ratio (mol %)	Mw (g/mol)	PDI	Conductivity (S cm^{-1})
L-PTEB	1:4	3700	2.3	2.5×10^{-2}
H-PTEB	1:2	5100	2.1	3.0×10^{-2}

Sample ID	PTEB:EDOT Weight Ratio (wt %)	Concentration of PTEB in Water (g/L)	Conductivity (S cm^{-1})
L-PTEB1	0	0.0	0.2
L-PTEB2	1	0.3	1.5
L-PTEB3	5	1.5	3.5
L-PTEB4	10	3.0	4.0
H-PTEB1	0	0.0	0.2
H-PTEB2	1	0.3	1.2
H-PTEB3	5	1.5	2.7
H-PTEB4	10	3.0	2.8

them. The solution covered copper grids were slowly dried by exposure to air. TEM was performed on a JEOL 1230EX operating at 120 kV with Gatan Dual Vision CCD camera.

RESULTS AND DISCUSSION

Synthesis and Characterization of PTEB

In a typical emulsion polymerization, surfactants play significant roles by forming micelles as the polymerization loci for the nucleation of particles as well as stabilizing the particles. In the current study, we proposed to use PTEB as a surfactant for the synthesis of PEDOT composite nanoparticle. PTEB was synthesized in a three-step procedure from its monomer, 2-(3thienyl)-ethoxy-4-butylsulfonate as first described by Tran-Van et al.[39] We followed the same procedure as shown in Figure 1 and synthesized two different molecular weight of PTEBs denoted as L-PTEB and H-PTEB for the low and high molecular weight PTEB, respectively, by adjusting the molar ratio of its monomer to the oxidant FeCl$_3$. The characteristics of L-PTEB and H-PTEB are shown in Table 1.

The effect of molecular weight of PTEB on its optical and thermal properties as measured by UV–VIS, DSC, and TGA techniques is shown in Figure 3(a–c). UV–VIS characterization of the two polymers gives an absorption band at 405

and 420 nm for L-PTEB and H-PTEB, respectively, in water solution corresponding to the π–π* electronic transition. The red-shifting of the absorption maximum demonstrates that with increasing molecular weight, the conjugation length of PTEB increases. The result is consistent with literature work that shows the conjugation length of conductive polymers increases with increasing molecular weight up to a certain molecular weight of the polymer.[42] DSC measurement [Fig. 3(b)] of the two polymers shows that both polymers exhibit T_g at 40 °C and no melting transition was observed up to temperature of 160 °C. TGA thermograms were recorded under nitrogen atmosphere for the two PTEBs. A drastic weight loss was observed in the temperature range 200–250 °C for L-PTEB and 250–300 °C for H-PTEB followed by a continuous gradual weight loss. Such a massive weight loss in the temperature range between 200 and 300 °C (>50 wt %) should be related to the decomposition of side chain containing sulfonate groups,[43] the removal of tetrabutylammonium, a counter ion to the sulfonate group of PTEB, as well as the degradation of polythiophene backbone of PTEB.[35] Similar thermal property was also observed in poly (3-alkyl thiophene) system.[44] However, the onset temperature of 5% weight loss is much lower for PTEB than those for poly(3-alkyl thiophene)s. This is attributed to the presence of alkoxy pendant groups which makes the system more reactive and easily to be
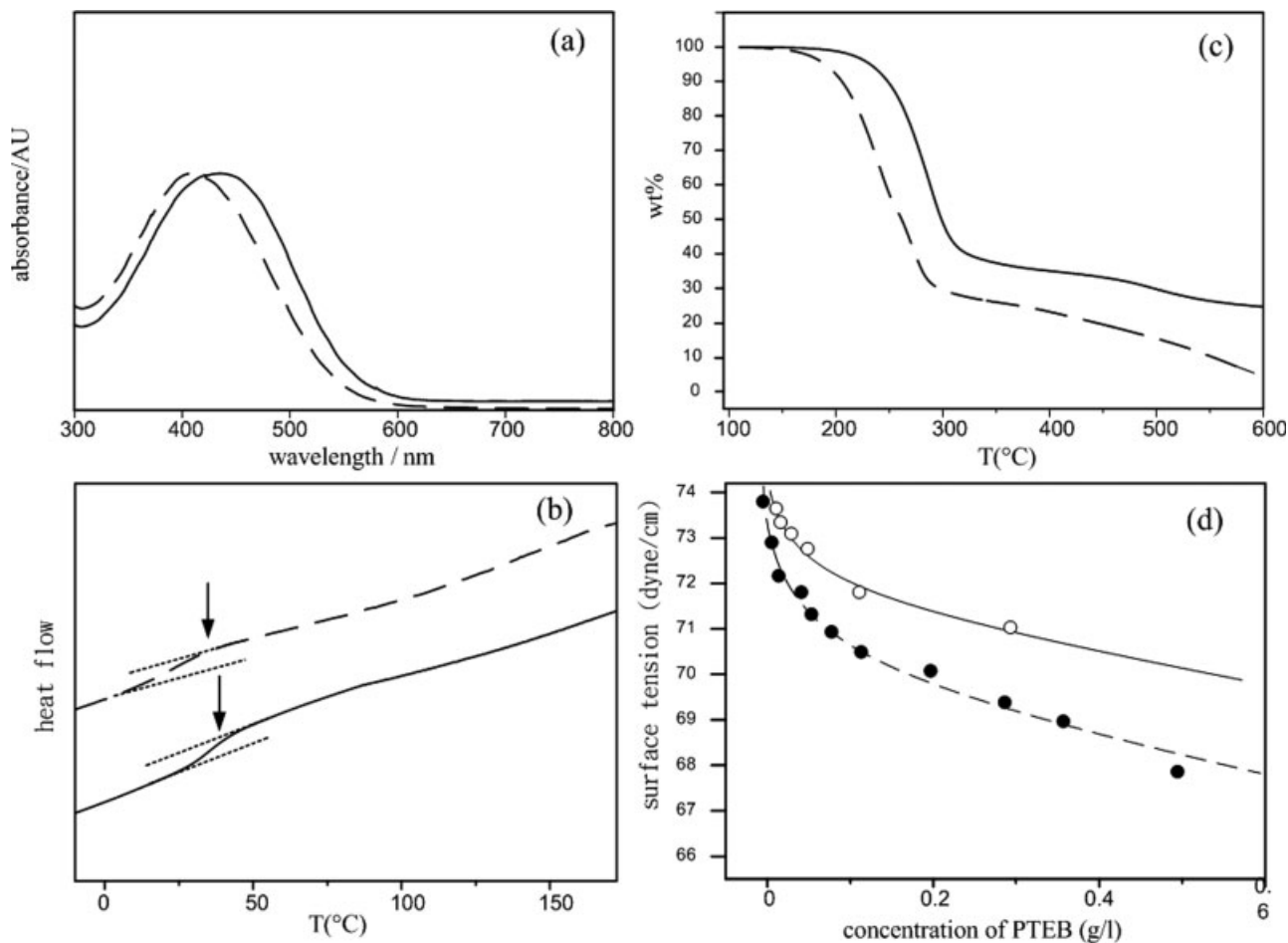
Figure 3. (a) UV–VIS absorption of PTEB in aqueous solution. (b) The thermal transition of PTEB is measured by using DSC. (c) The thermal stability of PTEB is measured as the weigh loss versus temperature using TGA. (d) Surface tension of PTEB aqueous solution is measured as a function of PTEB concentration in water. L-PTEB (– –) and H-PTEB (—).

oxidized as well as to the presence of sulfonate functional groups which is known for their lower thermal stability. The second weight loss step, which took place in the temperature range of 300–600 °C corresponds to the further degradation of polymer backbone leaving a char yield of 10 and 30% for L-PTEB and H-PTEB, respectively. In addition, the onset temperature of 5% weight loss for the polymer is found to increase with increasing molecular weight. This decreasing thermal stability with the decreasing molecular weight is expected for it has been observed in many polymer systems. The relatively poor thermal property of PTEB may prevent it from being used as a pure material in many optoelectronic applications that require high temperature annealing. We will show later that by incorporating PTEB into PEDOT, the thermal

property of the composite particles is much improved.

To further test the surfactant efficiency of PTEB used in the subsequent emulsion synthesis, we measured the surface tension as a function of different concentrations of PTEB. Figure 3(d) shows that measured surface tension as a function of PTEB concentration in water for both PTEBs. The surface tension for both PTEB solutions decrease monotonically with increasing PTEB concentrations. For the same concentration, the surface tension of L-PTEB solution is slightly lower than that of H-PTEB. Within this concentration range, a critical micelle concentration (CMC) for both surfactant solutions was not observed from the surface tension measurement. For emulsion polymerizations, typically, three mechanisms of particle nucleation are discussed:

droplet nucleation, homogeneous nucleation, and micellar nucleation. For all subsequent emulsion polymerization, the concentrations of PTEB were below its CMC; for example, no micelle was present in the polymerization solution. Therefore, for the subsequent emulsion polymerization, the location for particle nucleation is primarily from the mechanism of homogeneous nucleation.

Synthesis of PEDOT/PTEB Latex Particles

The synthesis of PTEB/PEDOT composite latex particles follows a standard emulsion polymerization method in which a radical polymerization starts with water, monomer, and surfactant. The synthesis scheme is shown in Figure 1. An aqueous surfactant solution was prepared with different amount of PTEB in 100 mL of deionized water under stirring. Since EDOT is almost insoluble in water (2.1 g/L at room temperature), EDOT (3.1 g, 22 mmol) was first added in 5 mL methanol and the solution was then added in the surfactant solution with stirring. The amount of PTEB added into the final aqueous solution was adjusted so as to make PTEB concentration of 0, 0.3, 2.1, and 3.0 g/L in water and to make weight ratio PTEB to EDOT of 0, 0.01, 0.07, 0.1 wt %, respectively. The oxidant $Fe(OTs)_3$ (29.8 g, 44 mmol) was added slowly into the mixture with a molar ratio of $Fe(OTs)_3$ to EDOT = 1/2 for polymerization and the solution was stirred for 3 days at room temperature. The initially greenish polymerization solution gradually turns bluish. After filtration, the precipitate is washed with deionized water and dried. To remove unreacted monomer, oxidant and excess PTEB, the precipitate is then again dispersed in methanol, ultrasonicated for 10 min and washed for purification.

The effect of surfactant concentration of H-PTEB on the morphology of the composite latex particles is shown in Figure 4(a–d). TEM studies show that the PEDOT particles synthesized without any PTEB surfactant were large and of irregular shape with a typical particle size larger than 1 μm [see Fig. 4(a)]. At a relatively low loading of 1 and 5 wt % PTEB (see sample H-PTEB2 and H-PTEB3 in Table 1), smaller but still irregular-shaped PEDOT:PTEB composite particles were synthesized as shown in Figure 4(b,c). At highest loading (10 wt %, H-PTEB4), TEM studies show that latex particles become spherical in shape and the average size of the particles are in the range of 100 nm as shown in Figure 4(d).

However, most spherical particles are connected to each other, indicating H-PTEB at this concentration is not as effective for particle separation. By comparison, the effect of L-PTEB on the morphology of the latex particles is much more pronounced. Figure 4(e–h) show that with increasing L-PTEB concentration, the morphology of the latex particles synthesized changes from irregular-shape to perfectly spherical particle even at low concentration compared with that of H-PTEB. The fact that spherical latex particles with L-PTEB were synthesized indicates that the growing latex particles during polymerization were swelled by monomers and/or oligomeric radicals. In addition, each particle was separated from each other as shown in Figure 4(g,h). Therefore, L-PTEB was more effective in stabilizing particle against coagulation.

Property of PEDOT:PTEB Latex Particles

Thermal Gravimetric Analysis

The thermal stability of conducting polymers is critical for their potential industrial application. TGA is an important dynamic method to detect the degradation behavior of the synthesized nanoparticles. The thermal stability of PEDOT:PTEB latex nanoparticle was measured by using TGA. Figure 5(a,b) show the weight loss of latex samples synthesized with L-PTEB and H-PTEB, respectively, as a function of temperature. As was discussed previously, both pure L-PTEB and H-PTEB have relatively poor thermal stability with dramatic weight loss above 200–300 °C. However, the latex samples synthesized with PTEB surfactant shows significant improvement in the degradation temperature even with 1 wt % of PTEB to EDOT monomer. For latex particles synthesized with L-PTEB or H-PTEB, the degradation temperature and the char yield increase significantly with increasing PTEB to EDOT monomer. Combined with the result from TEM measurement, the improvement in the thermal property is likely attributed to the higher molecular weight of PEDOT chains synthesized as well as better PEDOT crystalline phase formation in the particle due to the presence of PTEB. Without 1 wt % PTEB as surfactant in the emulsion polymerization, only lower molecular weight of PEDOT were synthesized and these PEDOT form aggregates and show poor thermal property. With 5 and 10 wt % L-PTEB
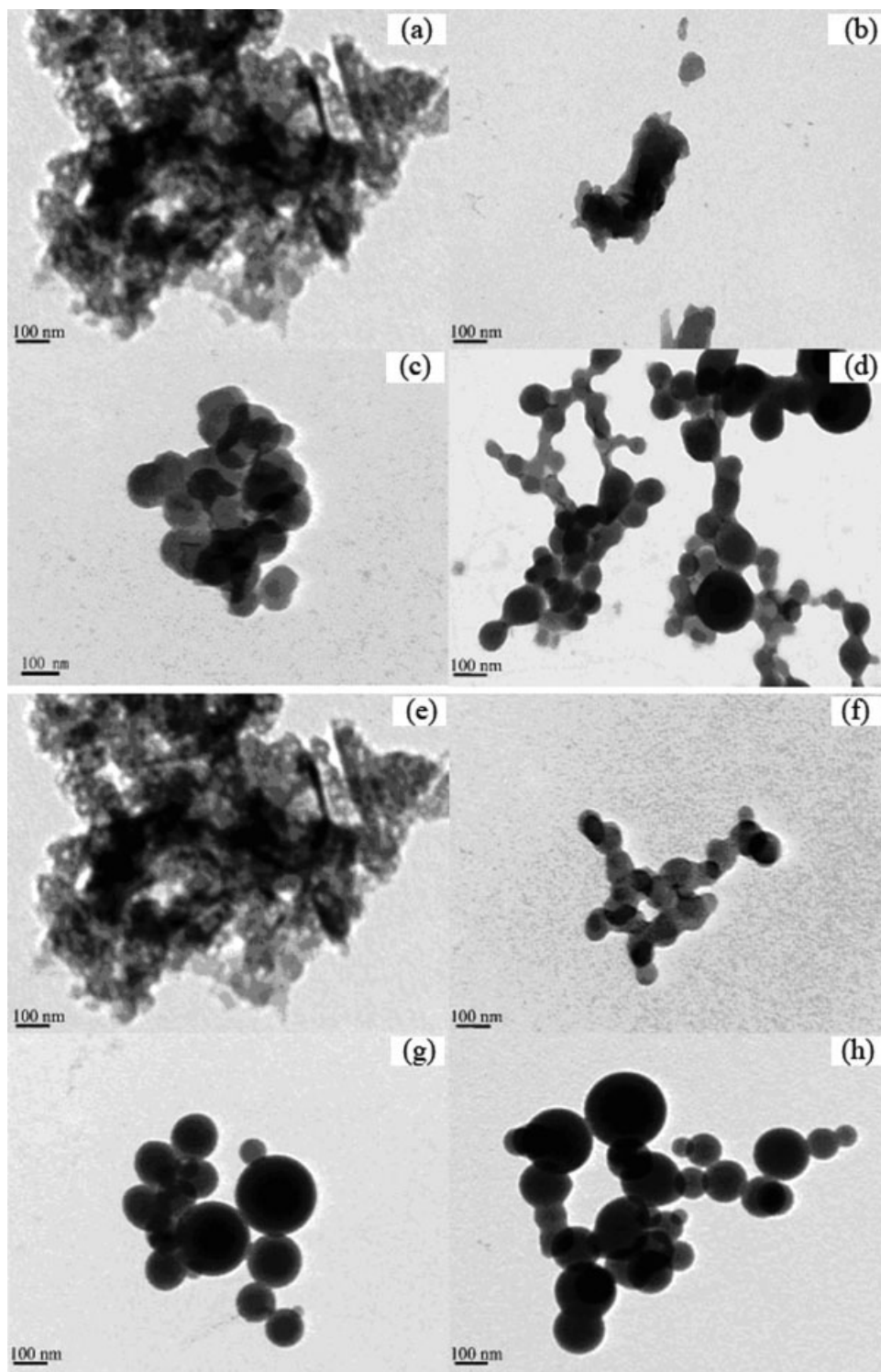
Figure 4. TEM micrographs of PEDOT:H-TEB latex particles for different weight fraction of PTEB to EDOT. (a) 0, (b) 1, (c) 5, and (d) 10 wt % of H-PTEB to EDOT; (e) 0, (f) 1, (g) 5, and (h) 10 wt % of L-PTEB to EDOT.

to EDOT in polymerization solution, the char yield is larger than that of nanoparticles synthesized with H-PTEB. This result is consist-

ent with TEM measurement. The nanoparticles synthesized with L-PTEB are spherical shape indicating those particles grow by absorption of
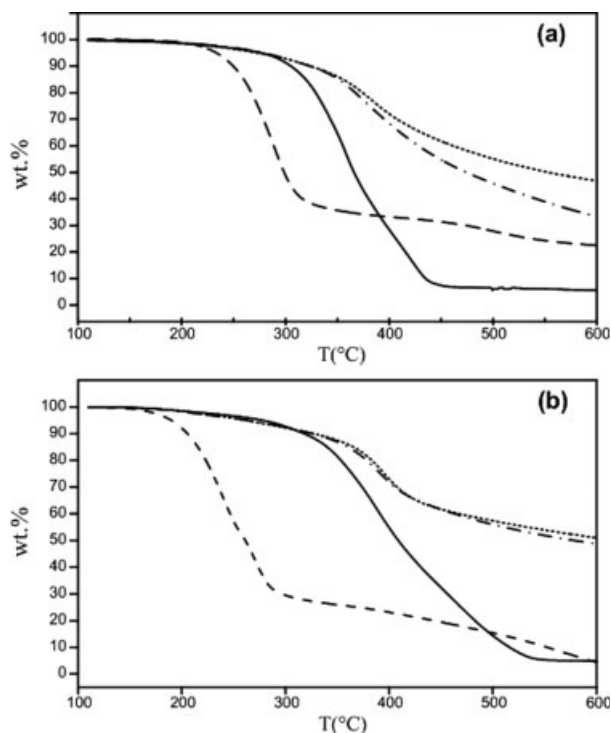
Figure 5. Thermogravimetric analysis of (a) PEDOT:H-PTEB and (b) PEDOT:L-PTEB latex particle with different amount of initial PTEB. (– – –) pure PTEB, (——) 1 wt %, (–·–·–·–) 5 wt %, and (······) 10 wt %.

oligomeric radicals which increases the molecular weight of PEDOT chains synthesized.

Conductivity

Figure 6 shows the effect of the PTEB addition to EDOT on the conductivity of the PEDOT:
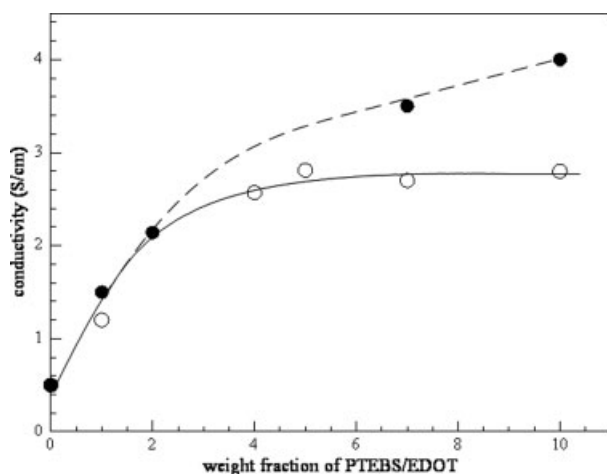
Figure 6. Conductivity of PEDOT:H-PTEB (——) and PEDOT:L-PTEB (– – –) for different amount of PTEB.

PTEB coated films. Without any PTEB, the conductivity of PEDOT film was found to be around 0.5 S/cm. With increasing concentration of H-PTEB, the conductivity of the PEDOT:PTEB film increases. However, at 5 wt % of H-PTEB to EDOT monomer, the conductivity of PEDOT:H-PTEB films saturate around 2.5 S/cm which is ~5 times increase from that of the pure PEDOT film. For nanoparticles synthesized with L-PTEB, the conductivity increases with increasing PTEB. The maximum conductivity achieved in this study with 10 wt % of PTEB is close to 4 S/cm. The improvement of conductivity of PEDOT:L-PTEB may be due to better surfactant property of L-PTEB which yields higher molecular weight of PEDOT particle synthesized.

UV–VIS Measurement

The UV–VIS spectra of the latex particles prepared under different concentration of PTEB were illustrated in Figure 7(a,b) for H-PTEB and
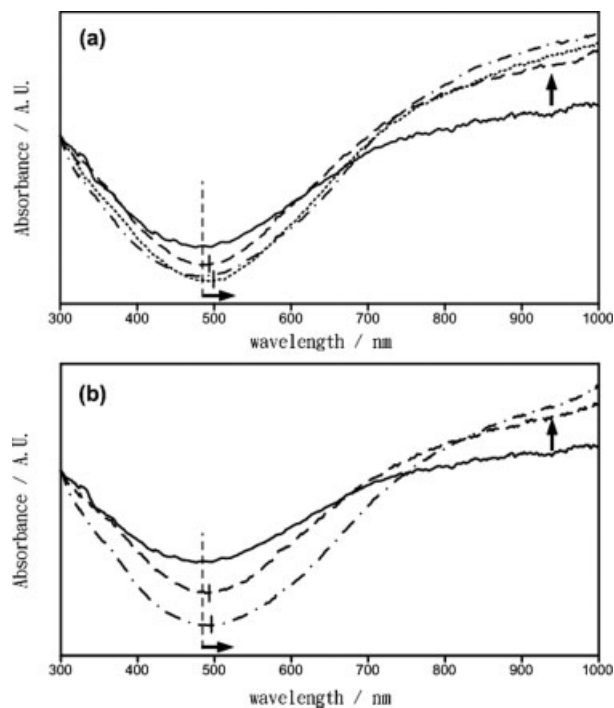
Figure 7. UV–VIS measurement of (a) PEDOT:H-PTEB and (b) PEDOT:L-PTEB latex particle with different amount of initial PTEB. (——) 0 wt %, (– – –) 1 wt %, (–·–·–·–) 5 wt %, and (········) 10 wt %. The vertical dash line indicates the onset of absorption of pure PEDOT and the short vertical solid line indicates the shift in the onset of the absorption of PEDOT:PTEB.

L-PTEB, respectively. The trend of absorption curves are the same for all PEDOT:PTEB films prepared with different amount of PTEB which shows that the absorption around 500 nm decreases while the absorption >700 nm increases with increasing PTEB. In Figure 7, the vertical dash line denotes the onset of absorption of pure PEDOT and the short vertical solid line denotes the shift in the onset of the absorption of PEDOT:PTEB film. The red-shifting of the onset absorption indicates that PEDOT was doped with the sulfonate groups of PTEB which results in longer conjugation length of PEDOT. The UV–VIS measurement of PEDOT:PTEB films correlate qualitatively well with the conductivity measurement.

FTIR

To give a deeper insight of the change in the chemical structure upon PTEB doping, we performed FTIR measurement on PEDOT:PTEB film. Figure 8(a,b) shows the changes in the FTIR spectra of PEDOT:PTEB powders prepared with H-PTEB and L-PTEB, respectively. Note that the vibrations at around 1336–1519 cm^{-1} are due to C—C or C=C stretching of quinoidal structure of thiophene ring and due to ring stretching of thiophene ring (benzoidal structure), respectively. Vibration at 1186, 1139, and 1080 cm^{-1} are related to ether bond stretching in the ethylene dioxy group. The band at around 1336 cm^{-1}, which indicates the existence of the quinoidal structure, is observed for all of the pure PEDOT and PEDOT:PTEB composite latecies. Therefore all of particles synthesized are well-doped PEDOT. However, for both H-PTEB and L-PTEB, the peaks at 1186, 1336, and 1519 cm^{-1} are shifted toward higher wave number with the addition of PTEB into PEDOT. This result is distinctly different from that of PEDOT prepared with emulsion polymerization using different oxidant and emulsifier.[33] In their study, upon doping those peaks are shifted to a lower wave number. They argued that the shift is due to a higher degree of p-doping achieved in the polymerization. In our system, upon doping of PTEB those peaks shifted toward higher wave number suggest an intermolecular interaction between PTEB with the corresponding chemical structure. Therefore, the FTIR measurement shows that PTEB can be incorporated into PEDOT particle during polymerization as well as effectively serves as dopant for PEDOT.
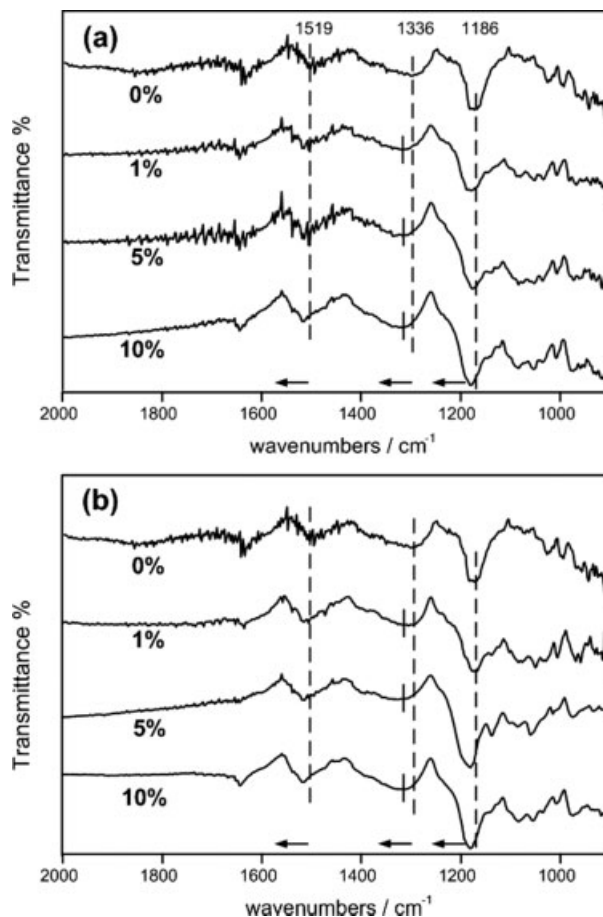
Figure 8. FTIR measurement of (a) PEDOT:H-PTEB and (b) PEDOT:L-PTEB for different amount of initial PTEB. The short vertical solid line indicates the shift in the wavenumber associated with stretching of quinoidal structure (~1336 cm^{-1}) of PEDOT:PTEB compared with that of pure PEDOT (vertical dash line).

Structure Determination Using X-ray

X-ray diffraction patterns of PEDOT:PTEB composite nanoparticles obtained from H-PTEB and L-PTEB systems are shown in Figure 9(a,b), respectively. We believe that these X-ray diffraction patterns can prove PTEB intercalation doping to PEDOT. Previously, X-ray analysis of PEDOT films synthesized with Fe(OTs)$_3$ shows that the corresponding crystal structure of its film is of the orthorhombic type with diffraction peaks 2θ ~6.1°, 12.1°, and 25.8°. These diffraction peaks correspond to (1 0 0), (2 0 0), and (0 2 0) reflections with the lattice parameter a = 14.3 Å, b = 6.8 Å and c = 7.8 Å of the PEDOT crystal.[45] In addition, a detailed structural analysis showed that the constant a corresponds to
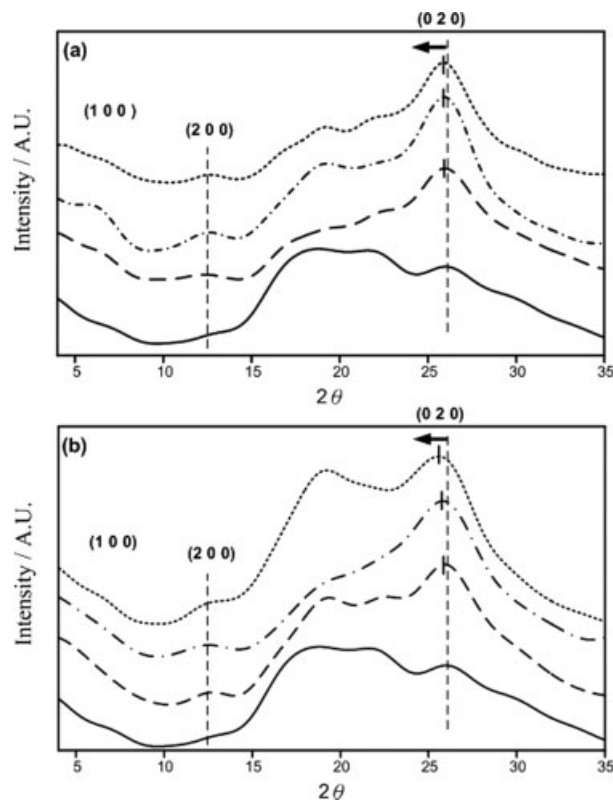
Figure 9. X-ray spectrum of (a) PEDOT:H-PTEB and (b) PEDOT:L-PTEB for different amount of PTEB: (———) 0 wt %, (– – –) 1 wt %, (—·—·—) 5 wt %, and (······) 10 wt %. The short vertical solid line indicates the shift in the distance of the (0 2 0) reflection in PEDOT:PTEB compared with that in pure PEDOT (vertical dash line).

the interchain distance between PEDOT backbone in the unit cell. The constant c value of the unit cell is related to the repeat unit of PEDOT chain which was previously measured by Aasmundtveit et al.[45] PEDOT chains stack on top of each other with a stacking distance of $b/2$. In Figure 9(a,b), the results of our X-ray measurement showed that without PTEB, pure PEDOT samples are mainly amorphous, whereas the PEDOT:PTEB samples show their characteristic diffraction peaks, which are indicative of the existence of crystalline phase. The change in the chain structure induced by PTEB provide one of explanations of the different conductivities of PEDOT:PTEB. Since the increase in the crystallinity of conducting polymer reduces the conjugation defects occurring in the system, therefore, in general, for conducting polymer the system becomes more conductive if the molecular order, for example, as in crystalline phase is increased.

In addition to a more intense peak corresponding to the (0 2 0) reflection plane, this peak position of the PEDOT:PTEB latex is shifted from 25.8° to lower angle with increasing PTEB. The amount of angle shifted increases with increasing PTEB added in the latex for both H-PTEB and L-PTEB systems. The shift to a lower angle of the (0 2 0) reflection plane in X-ray diffraction patterns corresponds to an increase in the stacking distance of PEDOT chains. This result is, however, dramatically different from that of PEDOT synthesized with $Fe(OTs)_3$ and smaller molecule emulsifier like DBSA (dodecylbenzene sulfonic acid).[35] The increase in conductivity of PEDOT induced by organic solvent treatment also showed an increase of the (0 2 0) diffraction peak position which in turn corresponded to a decrease in the stacking distance upon doping.[46] In our present study, the decrease in (0 2 0) peak position, therefore the increases in stacking distance in b direction must indicate that the stacked layers of PEDOT crystal are separated by layers containing PTEB. In addition, upon intercalating into the stacked layers of PEDOT, PTEB also serves as a dopant for the PEDOT which results in the increase in the conductivity with increasing PTEB concentration in the emulsion polymerization.

The growth mechanism of PEDOT nanoparticles with PTEB as conducting surfactant is summarized. Figure 10(a,b) shows a schematic representation of nucleation and growth process of PEDOT without or with PTEB, respectively. For the emulsion polymerization without PTEB as surfactant, as PEDOT grows in chain length, it becomes highly insoluble in water and unstable to suspend in water. Therefore, oligomeric PEDOT chains coagulate with each other forming large aggregates consisting of small nuclei or particles as shown in Figure 10(a). For the emulsion polymerization with PTEB, the particle growth mechanism is dramatically different. As oligomeric PEDOT grows in chain length, it absorbs onto PTEB and the composite particle is stabilized in polymerization solution due to surfactant property of PTEB. Stabilized particles can grow in size by the absorption of more oligomeric radicals and/or more PTEB. Because of the increase in the hydrophilicity inside the growing particles, monomeric and oligomeric PEDOT radicals and PTEB swell the growing particle, resulting in the formation of spherical particle. This process is evident from the TEM
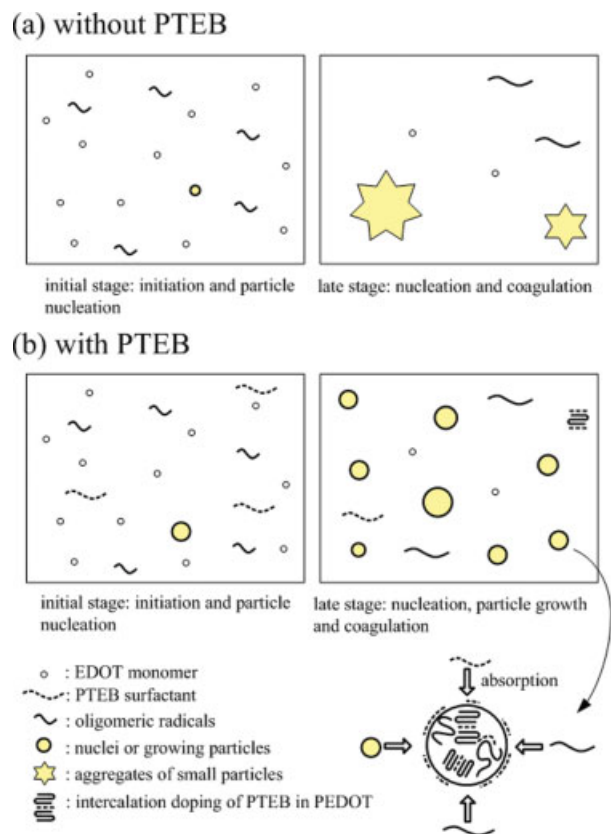
Figure 10. Schematic of the growth mechanism of PEDOT:PTEB particle (a) without PTEB and (b) with PTEB. With PTEB surfactant, the growing PEDOT: PTEB particles absorb PTEB, oligomeric radicals of PEDOT resulting in the swelling of the particles. PTEB serves as intercalating dopant as well as colloid dispersant. [Color figure can be viewed in the online issue, which is available at www.interscience. wiley.com.]

measurement. Lastly, from our UV–VIS, FTIR, and X-ray measurements, we found that PTEB is effectively intercalated into the PEDOT crystal as well as serves as dopant for PEDOT.

CONCLUSIONS

In this article, fully conducting latex nanoparticles with high conductivity were synthesized by emulsion polymerization using water soluble conducting polymer as surfactant. The addition of PTEB in the latex plays two roles, surfactant for stabilizing the PEDOT nanoparticles and dopant for the enhancement of its conductivity. With increasing PTEB incorporation in the latex, thermal stability, and crystallinity of PEDOT increase. Smaller and spherical

PEDOT:PTEB nanoparticles with diameter <100 nm can be synthesized with increasing amount of PTEB added during the emulsion polymerization. TGA measurement shows that the thermal degradation temperature of the latex increases considerably with increasing amount of PTEB in the latex. Evidence from UV–VIS and FTIR measurement showed that strong molecular interaction between PTEB and PEDOT resulted in the doping of PEDOT chains. X-ray analysis on the PEDOT crystal structure further demonstrated that PTEB chains were intercalated in the layered crystal structure of PEDOT. We proposed that alternating layers of PTEB and PEDOT were formed during particle growth in the emulsion polymerization. Contrary to nonconductive surfactant covered conductive nanoparticle, the conductivity of PEDOT:PTEB increases continuously with increasing PTEB surfactant concentration. Fully conductive film made from PEDOT:PTEB nanoparticles can be made with an improvement in conductivity closed to 10 times better than that of pure PEDOT. The present study provides a novel approach for synthesizing highly conductive and solution processable conducting nanoparticles for optoelectronic application.

REFERENCES AND NOTES

1. Groenendaal, B. L.; Jonas, F.; Freitag, D.; Pielartzik, H.; Reynolds, J. R. Adv Mater 2000, 12, 481.
2. Ha, Y. H.; Nikolov, N.; Pollack, S. K.; Mastrangelo, J.; Martin, B. D.; Shashidhar, R. Adv Funct Mater 2004, 14, 615.
3. Crispin, X.; Jakobsson, F. L. E.; Crispin, A.; Grim, P. C. M.; Andersson, P.; Volodin, A.; van Haesendonck, C.; Van der Auweraer, M.; Salaneck, W. R.; Berggren, M. Chem Mater 2006, 18, 4354.
4. Welsh, D. M.; Kumar, A.; Meijer, E. W.; Reynolds, J. R. Adv Mater 1999, 11, 1379.
5. Jonas, F.; Krafft, W.; Muys, B. Macromol Symp 1995, 100, 169.
6. Huang, F.; MacDiarmid, A. G.; Hsieh, B. R. App Phys Lett 1997, 71, 2415.
7. Kim, W. H.; Makinen, A. J.; Nikolov, N.; Shashidhar, R.; Kim, H.; Kafafi, Z. H. Appl Phys Lett 2002, 80, 3844.

8. Hadipour, A.; de Boer, B.; Wildeman, J.; Kooistra, F. B.; Hummelen, J. C.; Turbiez, M. G. R.; Wienk, M. M.; Janssen, R. A. J.; Blom, P. W. M. Adv Funct Mater 2006, 16, 1897.

9. Zhang, F.; Mammo, W.; Andersson, L. M.; Admassie, S.; Andersson, M. R.; Inganas, O. Adv Mater 2006, 18, 2169.

10. Yoon, H.; Chang, M.; Jang, J. Adv Funct Mater 2007, 17, 431.

11. Meskers, S. C.; van Duren, J. K. J.; Janssen, R. A. J.; Louwet, F.; Groenendaal, L. Adv Mater 2003, 15, 613.

12. Zhang, S.; Hou, J.; Zhang, R.; Xu, J.; Nie, G.; Pu, S. Eur Polym J 2006, 42, 149.

13. Sakai, N.; Prasad, G. K.; Ebina, Y.; Takada, K.; Sasaki, T. Chem Mater 2006, 18, 3596.

14. Kros, A.; van Hovell, W. F. M.; Sommerdijk, N. A. J. M.; Nolte, R. J. M. Adv Mater 2001, 13, 1555.

15. Richardson-Burns, S. M.; Hendricks, J. L.; Foster, B.; Povlich, L. K.; Kim, D. H.; Martin, D. C. Biomaterials 2007, 28, 1539.

16. Armes, S. P. Synth Met 1987, 20, 365.

17. Thompson, B. C.; Kim, Y.-G.; McCarley, T. D.; Reynolds, J. R. J Am Chem Soc 2006, 128, 12714.

18. Cabarcos, E. L.; Carter, S. A. Macromolecules 2005, 38, 4409.

19. Billingham, N. C.; Calvert, P. D. Adv Polym Sci 1989, 90, 1.

20. Smith, R. R.; Smith, A. P.; Stricker, J. T.; Taylor, B. E.; Durstock, M. F. Macromolecules 2006, 39, 6071.

21. Menon, R.; Yoon, C. O.; Moses, D.; Heeger, A. J. Handbook of Conducting Polymers; Marcel Dekker: New York, 1998.

22. Ouyang, J.; Xu, Q.; Chu, C.-W.; Yang, Y.; Li, G.; Shinar, J. Polymer 2004, 45, 8443.

23. Leclerc, M. Adv Mater 1999, 11, 1491.

24. Doherty, W. J.; Wysocki, R. J.; Armstrong, N. R.; Saavedra, S. S. Macromolecules 2006, 39, 4418.

25. Lefebvre, M.; Qi, Z. G.; Rana, D.; Pickup, P. G. Chem Mater 1999, 11, 262.

26. Ouyang, J.; Chu, C.-W.; Chen, F.-C.; Xu, Q.; Yang, Y. Adv Funct Mater 2005, 15, 203.

27. Huang, J.; Miller, P. F.; Wilson, J. S.; de Mello, A. J.; de Mello, J. C.; Bradley, D. D. C. Adv Funct Mater 2005, 15, 290.

28. Sotzing, G. A.; Reynolds, J. R.; Steel, P. J. Adv Mater 1997, 9, 795.

29. Khan, K. A.; Armes, S. P. Langmuir 1999, 15, 3469.

30. Seo, K. I.; Chung, I. J. Polymer 2000, 41, 4491.

31. Cutler, C. A.; Bouguettaya, M.; Kang, T.-S.; Reynolds, J. R. Macromolecules 2005, 38, 3068.

32. Zhang, X. Y.; Lee, J. S.; Lee, G. S.; Cha, D. K.; Kim, M. J.; Yang, D. J.; Manohar, S. K. Macromolecules 2006, 39, 470.

33. Lei, Y.; Oohata, H.; Kuroda, S.-I.; Sasaki, S.; Yamamoto, T. Synth Met 2005, 149, 211.

34. Mumtaz, M.; de Cuendias, A.; Putaux, J. L.; Cloutet, E.; Cramail, H. Macro Rapid Commun 2006, 27, 1446.

35. Choi, J. W.; Han, M. G.; Kim, S. Y.; Oh, W. G.; Im, S. S. Synth Met 2004, 141, 293.

36. Jang, J.; Oh, J. H. Adv Funct Mater 2005, 15, 494.

37. Riza, M.; Tokura, S.; Iwasaki, M.; Yashima, E.; Kishida, A.; Akashi, M. J Polym Sci Part A: Polym Chem 1995, 33, 1219.

38. Zhu, P. W.; Napper, D. H. J Colloid Interface Sci 1994, 164, 489.

39. Tran-Van, F.; Carrier, M.; Chevrot, C. Synth Met 2004, 142, 251.

40. Cui, L. L.; Xu, H.; He, P.; Sumitomo, K. K.; Yamaguchi, Y.; Gu, H. C. J Polym Sci Part A: Polym Chem 2007, 45, 5285.

41. Li, C. Y.; Chiu, W. Y.; Don, T. M. J Polym Sci Part A: Polym Chem 2007, 45, 3902.

42. Pokrop, R.; Verilhac, J.-M.; Gasior, A.; Wielgus, I.; Zagorska, M.; Travers, J.-P.; Pron, A. J Mater Chem 2006, 16, 3099.

43. Hietala, S.; Koel, M.; Skou, E.; Elomaa, M.; Sundholm, F. J Mater Chem 1998, 8, 1127.

44. Hu, X.; Xu, L. Polymer 2000, 41, 9147.

45. Aasmundtveit, K. E.; Samuelsen, E. J.; Inganas, O.; Petterson, L. A. A.; Johansson, T.; Ferrer, S. Synth Met 2000, 113, 93.

46. Kim, T. Y.; Park, C. M.; Kim, J. E.; Suh, K. S. Synth Met 2005, 149, 169.